Biogeosciences, 22, 5591–5605, 2025 https://doi.org/10.5194/bg-22-5591-2025 © Author(s) 2025. This work is distributed under the Creative Commons Attribution 4.0 License.





Mercury contamination in staple crops impacted by artisanal and small-scale gold mining (ASGM): stable Hg isotopes demonstrate dominance of atmospheric uptake pathway for Hg in crops

Excellent O. Eboigbe¹, Nimelan Veerasamy¹, Abiodun M. Odukoya², Nnamdi C. Anene³, Jeroen E. Sonke⁴, Sayuri Sagisaka Méndez⁵, and David S. McLagan^{1,6}

Wuse II, Abuja, 904101, Federal Capital Territory, Nigeria

Correspondence: David S. McLagan (david.mclagan@queensu.ca)

Received: 24 March 2025 – Discussion started: 8 April 2025

Revised: 23 June 2025 – Accepted: 9 July 2025 – Published: 20 October 2025

Abstract. This study investigates mercury (Hg) biogeochemical cycling and Hg uptake mechanisms in three common staple crops at a contaminated farm (Farm1) $\approx 500 \, \text{m}$ from an artisanal and small-scale gold mining (ASGM) processing site (PS) and a background farm (Farm2; $\approx 8 \, \text{km}$ upwind) in Nigeria. We examine air, soil, and various crop tissues using total Hg (THg), Hg stable isotope, Hg speciation, and methyl-Hg (MeHg) analyses.

Results show elevated gaseous elemental Hg (GEM) levels in the air (mean concentrations: $1200 \pm 400 \, \text{ng m}^{-3}$) and soil (mean THg concentration: $2470 \pm 1640 \, \mu \text{g kg}^{-1}$) at the PS, significantly higher than those at Farm1 (GEM: $54 \pm 19 \, \text{ng m}^{-3}$; THg: $76.6 \pm 59.7 \, \mu \text{g kg}^{-1}$), which are in turn significantly higher than those at the background site, Farm2 (GEM: $1.7 \, \text{ng m}^{-3}$; THg: $11.3 \pm 8 \, \mu \text{g kg}^{-1}$). These data confirm the ASGM-derived Hg contamination at the PS and the exposures of crops at Farm1 to elevated levels of Hg in both air and soil. Aligning with Hg concentrations in air and soil, Farm1 had significantly higher THg concentrations in all crop tissues compared to Farm2. At Farm1, foliage exhibits the highest THg concentrations in tissues, particularly for peanuts and cassava (up to $385 \pm 20 \, \mu \text{g kg}^{-1}$ in peanuts).

These data, along with highly negative δ^{202} Hg values in foliage and other crop tissues (indicative of light Hg iso-

tope enrichment imparted during stomatal assimilation of Hg) demonstrate atmospheric uptake of GEM as the primary uptake pathway for Hg in these crops. We observe air-to-foliage mass-dependent enrichment factors (ε^{202} Hg) of -2.60 ± 0.35 , -2.54 ± 0.35 , and $-1.28 \pm 0.43\%$ for cassava, peanuts, and maize, respectively. While our twoendmember mixing model shows that Hg in crop roots is influenced by both soil (59 %-74 %) and atmospheric (26 %-41 %) uptake pathways, we suggest soil Hg in roots is largely associated with the root epidermis/cortex (external root tissues) and that little soil-derived Hg is transferred to aboveground tissues (<7% across all crops). The lower THg concentrations in edible parts (with the exception of cassava leaves, commonly eaten in Nigeria) indicate that even translocation from foliage to other tissues is a relatively slow process. MeHg concentrations were < 1 % across all tissues, and probable daily intakes (PDIs) for both MeHg and THg based on typical diets in Nigeria were all below reference dose thresholds, indicating these crops are generally a lower health risk to the local population.

¹Dept. of Geological Sciences and Geological Engineering, Queens University, 36 Union St, Kingston ON, K7L3N6, Canada,

²Department of Geosciences, University of Lagos, G97X+XJC, Yaba, Oworonshoki, 101245, Lagos, Nigeria

³Ministry of Solid Minerals Development, Government of Nigeria, P.M.B. 107, Luanda Crescent,

⁴Géosciences Environnement Toulouse, CNRS/IRD/University of Toulouse, 14 Av. Edouard Belin, 31400, Toulouse, France

⁵Department of Environmental Sciences, University of Toronto, 1265 Military Trail, Toronto, ON, M1C1A4, Canada

⁶School of Environmental Studies, Queen's University, 116 Barrie St, Kingston, ON, K7L3N6, Canada

1 Introduction

Artisanal and small-scale gold mining (ASGM) is generally defined as mining activities related to the extraction of gold that involves minimal (or no) mechanization undertaken by individuals or small groups/cooperatives whose participation in these activities ranges from regulated to informal (illegal); specific definitions can vary between jurisdictions (Hentschel et al., 2002; Seccatore et al., 2014). In recent years, the ASGM sector has grown exponentially, driven by rising gold prices and the ease of selling gold (World Gold Council, 2024; Verbrugge and Geenen, 2019; Achina-Obeng and Aram, 2022). Currently, ASGM contributes $\approx 20 \%$ -30% of global gold production (PlanetGOLD, 2022), especially in emerging economies, where it serves as a vital source of livelihood for many communities. Despite attempts to regulate mercury (Hg) use in ASGM under the Minamata Convention (UNEP, 2013), elemental Hg (Hg(0)) use remains a fundamental part of gold processing in ASGM due to the effectiveness and simplicity of the Hg-gold amalgamation process (Veiga et al., 2006; Bugmann et al., 2022) and the general preference of miners for Hg amalgamation (Hinton et al., 2003; Jønsson et al., 2013).

ASGM is now considered the largest global source of anthropogenic Hg emissions (Streets et al., 2019; Munthe et al., 2019; Yoshimura et al., 2021). Recent estimates suggest that ASGM emits 838 ± 163 Mg of Hg to the air (almost entirely as gaseous Hg(0), or GEM) and releases $1221 \pm 637 \,\mathrm{Mg}$ of inorganic Hg forms, Hg(0) and divalent Hg (Hg(II)), to the land and rivers annually (Munthe et al., 2019). The continued rapid growth of the sector in the decade since the ratification and implementation of the Minamata Convention raises questions about the effectiveness of the measures introduced by the Convention in reducing the use and impacts of Hg in ASGM. Such concerns are largely driven by growth in illegal mining, a thriving illicit international trade market of Hg, and the criminal networks tied to both issues (Verité, 2016; Lewis et al., 2019; Marshall et al., 2020; Cheng et al., 2022). These security issues also present a major barrier to the implementation of more effective and holistic study of Hg use and impacts in ASGM areas (Moreno-Brush et al., 2020).

GEM has a long atmospheric residence time ($\approx 6-18$ months), and long-range atmospheric transport is the dominant mechanism for the global redistribution of Hg (Ariya et al., 2015). Hence, Hg emitted from sources such as ASGM can have impacts on human and environmental health in areas that are great distances from these activities (Bose-O'Reilly et al., 2010; Weinhouse et al., 2021). Work in recent decades has shown that terrestrial plants play a critical role in the global Hg cycle, acting as the primary sink of atmospheric Hg in terrestrial systems through the assimilation of GEM into foliar stomata during photosynthesis (a mechanism of GEM dry deposition) and subsequent storage within plant tissues (Jiskra et al., 2018; Obrist et al., 2021). This is observed in trees, grasses (e.g. Millhollen et al., 2006; Mao et

al., 2013; Assad et al., 2016), and crops such as rice, wheat, and corn (e.g. Niu et al., 2011; Yin et al., 2013; Sun et al., 2019). Total Hg (THg) concentrations in plant foliage (and other aboveground tissues) are proportional to local GEM concentrations (Millhollen et al., 2006; Fu et al., 2016; Sun et al., 2019; Wang et al., 2020). Another potential uptake pathway of atmospheric Hg in plants is sorption to and transfer through the foliage cuticle. However, wash-off by precipitation, revolatilization of sorbed Hg, and the likely slow transfer through the cuticle result in this uptake mechanism being minor compared to the stomatal assimilation pathway (Rea et al., 2000; Rutter et al., 2011a, b; Laacouri et al., 2013). While there is also potential for plants to take up Hg from soil via roots, a large body of research indicates that > 90 % of Hg in the aboveground biomass (AGB) of plants is derived from the air-foliage pathway, with the root epidermis/cortex providing an effective barrier for the less bioavailable forms of Hg found in soils (Beauford et al., 1977; Rutter et al., 2011b; Zhou et al., 2021). A major exception to this is the uptake of the more bioaccumulative and toxic methyl-Hg (MeHg) in species growing in saturated soils, such as rice (Qui et al., 2008).

Critical to the advancements that have been made in understanding the importance of this GEM uptake mechanism by vegetation is the use of Hg stable isotope analyses in air, plants, soils, and precipitation samples. Hg has seven stable isotopes, which undergo both mass-dependent fractionation (MDF) and mass-independent fractionation (MIF) in the environment (Blum and Bergquist, 2007). MDF occurs during biogeochemical transformations, while processes causing MIF are rarer and linked largely to photochemical processes and some dark abiotic reactions; both MDF and MIF enable researchers to track Hg sources and identify in situ transformation processes (Bergquist and Blum, 2009). For example, MDF is useful in tracking plant uptake, where foliage often shows large negative MDF shifts (-1% to -3%in δ^{202} Hg) during stomatal assimilation compared to the δ^{202} Hg isotope values of GEM in the surrounding air (Zhou et al., 2021, and references therein). After being taken up by leaf stomata, GEM is rapidly oxidized to divalent forms and can then translocate to other plant tissues, including stems, branches, bark, and seeds, supported by negative δ^{202} Hg values in stem and seeds that closely resemble values observed in foliage (Yin et al., 2013; Sun et al., 2019; Liu et al., 2021; McLagan et al., 2022a).

Significant gaps remain in our understanding of Hg uptake mechanisms, internal cycling, and associated health risks from Hg in crops, particularly as this relates to the largest global anthropogenic emitter of Hg: ASGM. The limited number of studies examining Hg in crops affected by ASGM activities have primarily focused on THg and occasionally also MeHg analyses, which may not fully capture the complexity of Hg dynamics in these systems. In addition, such studies have typically assumed soil—root to be the dominant

Hg uptake mechanism (Suhadi et al., 2021; Addai-Arhin et al., 2023).

In this study, we employ a multidisciplinary total-systems approach to comprehensively examine the dominant Hg uptake pathway and internal translocation and storage of Hg in three staple crops in a Nigerian farm adjacent to ASGM activities. Air, soil, and a range of crop tissues (foliage, stems, roots, and tubers/grains) were assessed using a series of Hg analyses (THg, MeHg, Hg stable isotopes, and Hg speciation) to provide critical data on the biogeochemical cycling of Hg in agricultural regions impacted by ASGM and preliminary assessment of the potential risks to human health from consuming these crops.

2 Methods

Methods described in this section are abbreviated due to the need for conciseness and the broad multidisciplinary approach utilized. Full details of the study site, sampling approaches, analytical methods, and quality assurance and quality control (QAQC) are provided in the Supplement.

2.1 Study area

The study is based around a mine $(8.87126^{\circ} \, \text{N}, 7.71828^{\circ} \, \text{E})$ and ASGM processing site (PS) $(8.9012^{\circ} \, \text{N}, 7.7061^{\circ} \, \text{E})$ separated by $\approx 3.5 \, \text{km}$ and situated near the town of Uke (population $\approx 20\,000$) in the Karu Local Government Area of Nasarawa State, $\approx 51 \, \text{km}$ southeast of Abuja, the capital city of Nigeria (Fig. 1). ASGM in this area began around 2015 following the discovery of gold, which attracted a significant influx of miners, and includes mining, ore processing with Hg, and amalgam burning (further details of the ASGM activities are described in Sect. S1 in the Supplement).

In July 2023, sampling was conducted at three sites: (1) the ASGM processing site (PS); (2) Farm1, situated $\approx 0.5 \text{ km}$ north of the processing site; and (3) Farm2, a control farm located ≈8 km north-northwest of the processing site in another town with no known sources of Hg, ASGM, or otherwise (Fig. 1). Predominant winds in this region are from the west-southwest (Iorhemba and Mijinyawa, 2021); thus, there is potential for emissions from the processing site to impact Farm1 (but unlikely to influence Farm2). Critically, Farm1 is on the opposite side of a small river to the processing site to ensure surface or groundwater flows from the processing site were not contaminating the Farm1 soils. We note that the informal nature of ASGM restricted sampling to the scope outlined below, and this was by invitation and was an allowable concession of the operators of the legally operating site, local and national governmental authorities, and the farmers themselves. This particularly limited the number of Hg stable isotope samples that could be collected for each crop and crop tissue type.

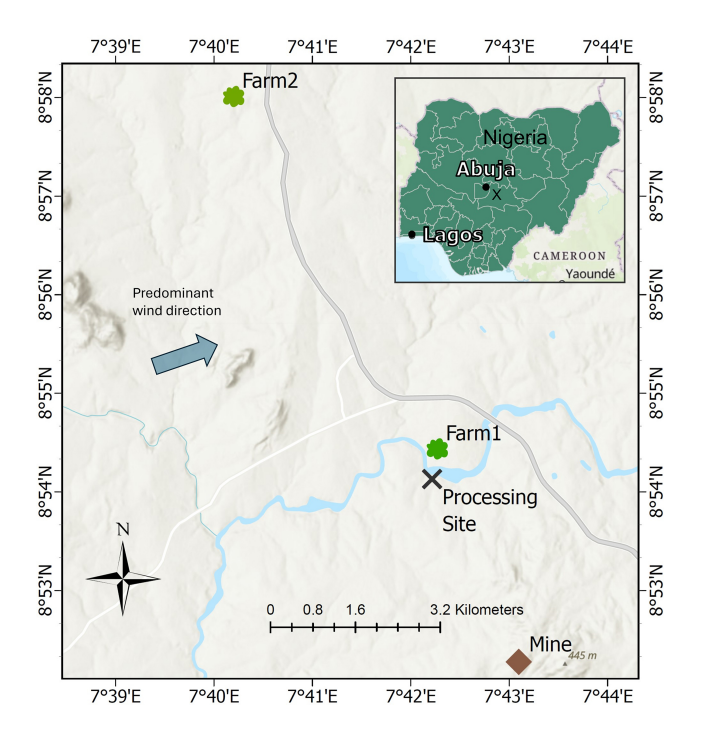


Figure 1. Map of the study area showing the mine, processing site (PS), Farm1, Farm2, and predominant winds in the region (Iorhemba and Mijinyawa, 2021). The inset map indicates major Nigerian cities, with the processing site marked by an "x" (Basemap: © OpenStreetMap Contributors 2025. Distributed under the Open Data Commons Open Database License (ODbL) v1.0).

2.2 Soil sampling

Surface soil samples (0-10 cm) were collected from the PS (n=13), Farm1 (n=8), and Farm2 (n=5) (farm soils were sampled directly around sampled plants) using standard sampling procedures (USEPA, 2023). Full details of the soil sampling procedures are provided in Sect. S2.

2.3 Air sampling

Considering the substantial emissions of Hg to air from ASGM and the potential for GEM uptake by vegetation (crops), it was critical to assess GEM concentrations. Hg passive air samplers (MerPAS samplers; Tekran Instruments Corp.) were deployed according to the guidelines of the developers (McLagan et al., 2016), and modifications were made for deployments in highly contaminated areas (shorter deployments and extreme care in sampler transport and storage) (McLagan et al., 2019; Si et al., 2020). MerPAS samplers were deployed for \approx 72 h at the PS (n = 3), \approx 144 h at Farm1 (n = 6), and \approx 100 d at (control) Farm2 (n = 1). See Sect. S2 for full details on MerPAS deployments (including blank details) and Table S7.1 for specific sampling periods.

2.4 Crop sampling

Foliage, stem, grains/tubers, and root samples of three crops cultivated at both Farm1 and Farm2 were collected: maize (Zea mays), cassava (Manihot esculenta), and peanuts (Arachis hypogaea). We note that, in cassava, tubers are true roots, but we classify "roots" as undeveloped (no tuber) adventitious roots/rootlets (Rees et al., 2012). Cassava and maize were nearing maturity at the time of sampling and \approx 1–2 months (or less) before harvest, while peanuts were fully mature and being harvested at the time of sampling. Three whole plants of each crop at each farm were removed from the soil for sampling, with care taken to consolidate belowground tissues with each selected plant. Due to sampling availability and access restrictions placed by farmers, the community, and mine owners, we could not deviate from this sample timing (and quantity). Full details of crop sampling procedures are provided in Sect. S2.

2.5 Analytical procedures

2.5.1 Solid-phase THg analyses

THg analysis for soil and plant samples (0.01–0.2 g aliquots) was carried out by thermal desorption, gold amalgamation, and atomic adsorption spectrometry according to USEPA Method 7473 (USEPA, 2007) using an MA-3000 direct Hg analyser (Nippon Instruments Corp.). All tissue and soil samples were measured in triplicate for THg, and full details of the analytical method are provided in Sect. S3. THg concentration analysis of MerPAS samples also utilized the MA-3000 direct Hg analyser (with ≈ 0.1 g additions of precleaned sodium carbonate) and followed methods developed by McLagan et al. (2016) with some refinements (including a verified 400 °C maximum combustion temperature), detailed in Sect. S3. Calculations of GEM concentrations (ng m^{-3}) followed methods described by McLagan et al. (2016), and further details are provided in Sect. S3. MerPAS samples used for Hg stable isotope analyses of GEM were corrected for the MDF offset (measured δ^{202} Hg +1.1 \pm 0.2 %) as posited by Szponar et al. (2020).

Quality assurance and quality control (QAQC) were exercised using replication of all THg sample analyses (2–3 replicates) and regular (after every 10 sample runs) analyses of (matrix-matched) certified reference materials (CRMs) and the internal liquid Hg standard. All recoveries were within accepted ranges, and specific details on the CRMs used and recovery data are presented in Table S3.1. All data are presented on a dry-weight (dw) basis.

2.5.2 Hg stable isotopes: extractions and analyses

All samples analysed for Hg stable isotopes were trapped off the exhaust of the MA-3000 detector during solid-phase THg analyses of the same matrix for sample preconcentration. This required combining some tissue samples for each

crop species from individual plants at Farm1 due to low THg concentrations (Farm2 samples were not considered due to low concentrations and analytical capacities of the multi-collector inductively coupled plasma mass spectrometer (MC-ICP-MS)). The combust and trap method broadly followed methods by Enrico et al. (2021) and McLagan et al. (2022b) with some modifications. This method allows the accumulation of Hg from matrix-matched samples measured for solid-phase THg concentrations within a single 5 or 10 mL inverse aqua regia (3:1 concentrated HNO₃: HCl diluted to 40 % v/v with DI water) trap. The MA-3000 combustion method followed the matrix-specific methods described in Sect. S3. A heated (≈ 60 °C) polytetrafluoroethylene (PTFE) tube connected to a coarse frit gas dispersion sparger (6 mm outer diameter; modified to 25 cm length) was connected to the MA-3000 detector outlet. Trapping samples analysed for THg concentrations allows direct recovery testing between the measured THg solid-phase concentrations and the liquid-phase THg concentrations within the trap, which removes the uncertainty of assuming homogenous THg solid-phase concentrations. Any sample with recovery below 80 % was not considered for Hg stable isotope analyses due to concerns that losses during extraction/analyses could artificially induce isotope fractionations. Recoveries of all samples analysed for Hg stable isotopes are listed in Table S3.3. All samples were diluted to a 20 % acid strength (by volume) for Hg stable isotope analyses.

An online cold vapour generator (CETAC-HGX-200) was used to reduce Hg(II) in the trapping solutions into Hg(0)vapour by SnCl₂ (3 % weight per volume) in 1 M HCl). Using this system, gas-phase Hg(0) is then introduced into a MC-ICP-MS (Thermo-Finnigan Neptune) for analyses of Hg stable isotopes at the Observatoire Midi-Pyrenees (Toulouse, France). Full details of the instrument setup can be found in Sun et al. (2013). Sample isotope ratios were corrected for mass bias by sample-standard bracketing using NIST 3133 (Blum and Bergquist, 2007; Sun et al., 2013). Results are reported as δ values in per mil (%) by referencing to NIST 3133, representing Hg mass-dependent fractionation (MDF), while MIF is reported in "capital delta" notation (Δ), which is the difference between the measured values and those predicted by the kinetic MDF law using equations previously stated (Blum and Bergquist, 2007). The quality control of Hg isotope measurements was assessed by analysing ETH-Fluka and UM Almaden reference standards, and these data are presented in Table S3.3. Uncertainties on sample δ and Δ signatures were conservatively estimated as the larger of the 2standard-deviation uncertainties on weekly ETH-Fluka, UM-Almaden, or sample replicates (Table S3.3). Due to the limited number of Faraday cups on the Neptune MC-ICP-MS, analysis of ²⁰⁴Hg was preferred to ²⁰³Tl or ²⁰⁵Tl (used in some studies for mass bias corrections). However, we confirm this follows the same method implemented in Jiskra et al. (2021) (further discussion on this is provided in Sect. S3).

2.5.3 Hg speciation/fractionation analyses

Solid-phase speciation/fractionation analyses were performed using the pyrolytic thermal desorption (PTD) method developed by Biester and Scholz (1996) adapted for use on a Lumex 915M with PYRO-915+ Module (Lumex Instruments Corp.) by Mashyanov et al. (2017). Due to the inherent uncertainties and challenges in peak identification of Hg(II) species, these analyses are considered qualitative and complementary (McLagan et al., 2022b). Further details of this method are provided in Sect. S3.

2.5.4 Methyl-Hg (MeHg) Analyses

MeHg concentrations were determined using an isotope dilution method and followed methods described in Mitchell and Gilmour (2008). A detailed description of this method is provided in Sect. S3. All QAQC data for MeHg analyses are presented in Table S3.2.

2.6 Two-endmember mixing model to identify Hg sources within crops

A two-endmember mixing model was used to quantitatively determine source pathways for Hg in internal crop tissues according to Eq. (S1). The δ^{202} Hg values of foliage for each crop are used as the first endmember: air–foliage uptake pathway. Similarly, the soil–root endmember must be the δ^{202} Hg signature of Hg immediately after uptake to the roots. Hence, the mean δ^{202} Hg value for Farm1 soils minus the MDF of soil to shallow roots (roots above 150 cm) (ε^{202} Hg: -0.35) taken from Yuan et al. (2022) is used. Details of this two-endmember mixing model and the data used in the derivation of the endmembers are provided in Section S4.

2.7 Estimates of annual Hg dry deposition rates to crops

Hg(0) dry deposition rates ($F_{\text{Hg(0):AGB}}$; g km⁻²) via the foliar uptake pathway to the aboveground biomass (AGB) for each crop were calculated using Eqs. (S2) and (S3) adapted from Casagrande et al. (2020) with additions relating to the transfer of Hg to other aboveground tissues and the transfer to edible belowground parts (for peanuts and cassava). This was achieved using annual edible biomass yields and the fraction of Hg in tubers/nuts derived from a foliage-based two-endmember mixing model (Table 1). Details of these calculations are provided in Sect. S5.

2.8 Probable daily intake calculations

We also calculated the probable daily intake (PDI) of MeHg and Hg(II) using the method from Zhao et al. (2019) adapted for MeHg and Hg(II) and the concentrations measured in the examined crops and their mean dietary intake data for adults

in Nigeria. Specific equations and data used in these calculations and the PDI data generated are presented in Sect. S6.

2.9 Statistical analyses

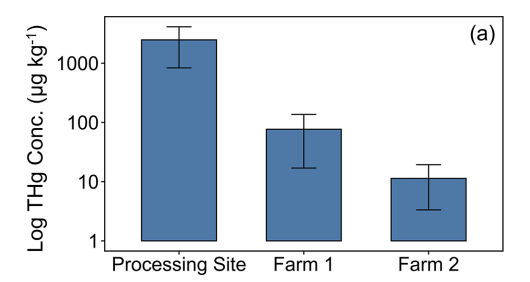
Statistical tests (Welch's *T* test; unequal variances and sample sizes) used to assess differences in THg concentrations and Hg stable isotopes, data analyses, and figures were all generated in RStudio (Boston, USA).

3 Results and discussion

3.1 Crop exposure levels: Hg concentrations in air and soils

Highly elevated GEM concentrations $(1200 \pm 400 \,\mathrm{ng}\,\mathrm{m}^{-3})$ were observed at the ASGM processing site (PS) (Fig. 2). These concentrations are $\approx 1000 \times$ background concentrations and consistent with levels observed in other ASGM regions where Hg is used in ASGM activities (González-Carrasco et al., 2011; Kawakami et al., 2019; Nakazawa et al., 2021; Snow et al., 2021) and indicate substantial Hg use and emissions at the PS. At Farm1 ($\approx 500 \,\mathrm{m}$ distance from the PS), GEM concentrations were significantly lower than at the PS (p = 0.014) but remained elevated ($54 \pm 19 \,\mathrm{ng}\,\mathrm{m}^{-3}$) above background, confirming exposure of Farm1 to GEM emissions from ASGM activities at the PS. In contrast, GEM concentrations at Farm2 ($1.7 \,\mathrm{ng}\,\mathrm{m}^{-3}$, n = 1) were consistent with the Northern Hemisphere background concentrations (≈ 1.5 – $2 \,\mathrm{ng}\,\mathrm{m}^{-3}$; Sprovieri et al., 2016).

Stable isotope measurements of GEM at sites exposed to elevated GEM concentrations were indicative of more negative MDF and more positive MIF signatures (PS: δ^{202} Hg, $-1.38 \pm 0.21\%$; Δ^{199} Hg, $0.07 \pm 0.03\%$. Farm1: δ^{202} Hg, $-0.94 \pm 0.19\%$; Δ^{199} Hg: $0.08 \pm 0.08\%$) (Fig. 4), which is typical of anthropogenic Hg emitted into the air from industrial (Sonke et al., 2010; Fu et al., 2021; McLagan et al., 2022b) and ASGM (Gerson et al., 2022; Szponar et al., 2025) sources. Considering that the burning of Hg-gold amalgams emits Hg(0) directly into the atmosphere, we deem the mean stable isotope values for Hg(0) in air in the contaminated areas (PS and Farm1) to be the signal most representative of the ASGM source. Contrastingly, GEM at Farm2 was relatively enriched in heavier isotopes and had a slightly negative MIF signal (δ^{202} Hg: $-0.01 \pm 0.19\%$; Δ^{199} Hg: $-0.12 \pm 0.08\%$), typical for GEM samples in background areas (Si et al., 2020; Szponar et al., 2020). We suspect that the rapid decline in GEM concentrations as we move away from the contamination source is influenced both by dilution with background air and by wind direction. Although GEM was not measured in areas downwind of the processing site, McLagan et al. (2019) observed a more gradual decline in GEM in areas downwind (compared to upwind sites) of a former Hg mine that remained heavily contaminated by elemental Hg; we suggest a similar pattern is likely at our study site. The vegetation



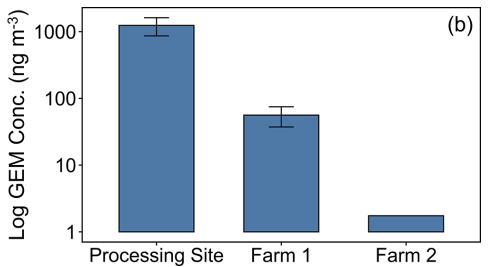


Figure 2. THg concentrations in soils (left; $\mu g kg^{-1}$) and GEM concentrations in air (right; $\eta g m^{-3}$) for all sampling sites.

of the area itself may play a role in reducing GEM concentrations around the ASGM area by removing GEM from the atmosphere during plant growing seasons. An assessment of this flux is described below in Sect. 3.4.

Similarly to GEM, soil samples at the PS were heavily contaminated (mean THg concentration: $2470\pm1640\,\mu g\,kg^{-1}$). Elevated soil Hg at the processing site is likely due to rapid GEM deposition from the atmosphere after emissions from amalgam burning and direct spills from improper handling of liquid Hg (Telmer and Veiga, 2009). The large variation in soil THg concentrations at this site (see Table S4.1) also reflects the spatial heterogeneity of processing activities at the PS, where Hg–gold amalgamation, ore washing, amalgam burning, and other activities occur.

Farm1 soils were also contaminated (mean THg concentration: $80.9 \pm 60.1 \,\mu g \, kg^{-1}$), but, similarly to differences in GEM concentrations, Farm1 was 1-2 orders of magnitude and significantly (p < 0.001) lower than the PS $\approx 500 \,\mathrm{m}$ away. Hence, we suggest emissions of GEM from the PS and deposition directly to soils or via GEM assimilation into vegetation, litterfall, and decomposition to be the dominant contamination pathway at Farm1, a mechanism now well described in the literature (Jiskra et al., 2015; Obrist et al., 2017; Zhou and Obrist, 2021). Our results fall into the range of concentration (2-5570 µg kg⁻³) recorded by Odukova et al. (2022) from farmlands adjacent to an ASGM region in Niger state of Nigeria and farms impacted by ASGM in Brazil $(81.7 \pm 13.5 \,\mu\mathrm{g\,kg}^{-1})$ (Casagrande et al., 2020). The latter study by Casagrande et al. (2020) is one of the only other studies examining Hg in ASGM-impacted agricultural areas directly attributing elevated concentrations in farm plants and soils to the atmospheric transfer pathway. In contrast, Farm2 soils were significantly lower again than Farm1 (p = 0.029) and at background levels with a mean concentration of $11.3 \pm 8.0 \,\mu\mathrm{g\,kg^{-1}}$.

All soil samples exhibited relatively small (compared to other contaminated soils) variation in δ^{202} Hg (PS: $0.29\pm0.98\%$; Farm1: $-0.26\pm0.43\%$ o) and Δ^{199} Hg MIF signal (PS: $-0.09\pm0.12\%$; Farm 1: $-0.07\pm0.03\%$ o) (Grigg et al., 2018; McLagan et al., 2022b; Vaňková et al., 2024). Nonetheless, the mean Δ^{199} Hg for GEM is slightly (but not significantly; p=0.073) higher than the mean value

for soils. This suggests minor evidence of some MIF induced by photochemical reduction from the soils (Rose et al., 2015).

3.2 Hg contamination and distribution in crops grown in ASGM-impacted areas

With the confirmation of exposure levels in both air and soils at Farm1 and Farm2 (control), it was then critical to assess the degree to which this contamination is affecting staple crops grown in this area and determine the predominant uptake mechanism of Hg in these plants. The mean THg concentrations in peanut (p = 0.021), cassava (p = 0.015), and maize (p = 0.004) tissues were all significantly elevated at Farm1 compared to Farm2 (Fig. 3 and Table S4.3). The highest THg concentrations were detected in the foliage of peanuts and cassava at Farm1 (peanut: $385 \pm 20 \,\mu g \,kg^{-1}$; cassava: $320 \pm 116 \,\mu g \,kg^{-1}$) and Farm2 (peanut: $7.06 \pm 2.74 \,\mu\text{g kg}^{-1}$; cassava: $13.2 \,\mu\text{g kg}^{-1}$) (Fig. 3), which suggests that the stomatal assimilation pathway is likely the dominant uptake mechanism of Hg in cassava and peanuts. While foliage THg concentrations were also elevated in maize (Farm1: $182 \pm 44 \,\mu\text{g kg}^{-1}$; Farm2: $5.16 \,\mu\text{g}\,\text{kg}^{-1}$), again demonstrating the likelihood of foliar Hg uptake, concentrations in maize roots were slightly higher (Farm1: $202 \pm 136 \,\mu\text{g kg}^{-1}$; Farm2: 5.74 ± 3.73) than foliage. Roots also had the second-highest concentration in peanuts and cassava. These data suggest potential for soilto-root Hg uptake in all three crops, but the contribution of the uptake mechanisms will be examined in more detail in Sect. 3.3.

Adjorololo-Gasokpoh et al. (2012) measured similar THg in cassava foliage (up to $177\,\mu g\,kg^{-1}$) and tuber (up to $185\,\mu g\,kg^{-1}$). Even though they did not observe any significant trends or differences between tissues, a novel component of their study was the division of cassava tuber into flesh, inner peel, and outer peel (Adjorololo-Gasokpoh et al., 2012). Division of root tissues into epidermis, cortex, and vascular bundle (or stele), followed by analysis for THg and stable Hg isotopes in crops impacted by ASGM, would provide critical insight into the effectiveness of the epidermis and/or cortex in restricting Hg uptake into the vascular bun-

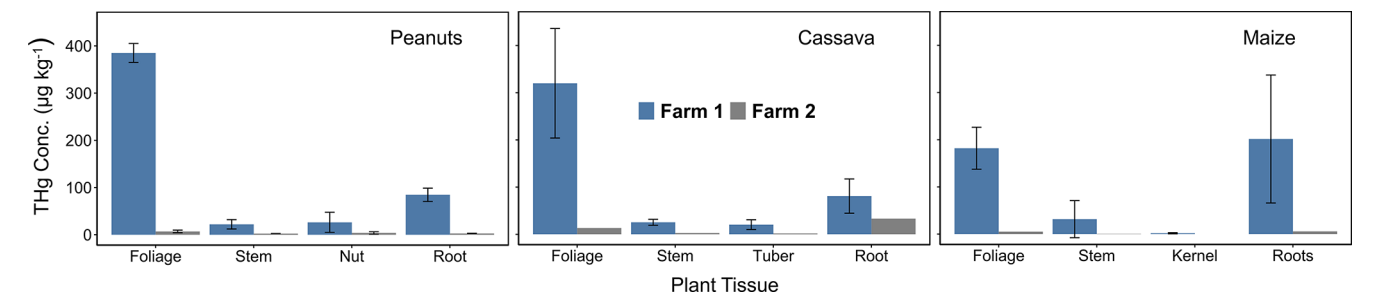


Figure 3. THg concentration ($\mu g kg^{-1}$) for all crop tissues at Farm1 and Farm2.

dle of inner root, as has been suggested elsewhere (Rutter et al., 2011b; Lomonte et al., 2014; Yuan et al., 2022).

Similar results showing the highest crop tissue THg concentrations in ASGM-affected farms are common in the literature (i.e. cassava in Golow and Adzei, 2002; cassava in Nyanza, et al., 2014; and soy (*Glycine max*) in Casagrande et al., 2020). However, we note the challenges of comparing absolute THg concentrations even of samples from the same species, as the distance from ASGM activities is likely a major determinant controlling observed levels of crop contamination, and, in many cases, little specific information on source–receptor distances is provided (i.e. Essumang et al., 2007; Adjorololo-Gasokpoh et al., 2012; Nyanza et al., 2014).

Of the three crops we studied, maize foliage exhibited lower THg concentrations than other crops, which may be attributed to maize's C₄ photosynthetic pathway. An earlier study by Browne and Fang (1983) found C₃ plants to take up 5 times more atmospheric Hg than C₄ species due to differences in leaf surface area, stomatal conductance (C3 plants exchange gases more readily with the atmosphere, allowing a greater uptake of atmospheric Hg), and internal resistance to Hg vapour uptake within the plant. Furthermore, maize kernels $(1.78 \pm 1.22 \,\mu\mathrm{g\,kg^{-1}})$ contained the lowest concentration in all crops at Farm1, suggesting minimal translocation from foliage or roots as observed by Wang et al. (2024), which again may be attributable to physiological differences in C₄ species – a hypothesis that requires direct exploration in future research. Glauser et al. (2022) also suggest that nonstomatal pathways can result in Hg sorption in certain maize tissues, such as maize tassels and silk. Although cassava is an intermediate between C4 and C3 plants, exhibiting some properties of both C₃ and C₄ photosynthetic pathways (El-Sharkawy and Cook, 1987; Bräutigam and Gowik, 2016; Xia et al., 2023), THg concentrations in cassava were higher than those in maize. This phenomenon is, however, not yet fully understood and warrants further research.

The concentration patterns for the crops were as follows: for maize, roots > foliage > stem > kernel; for peanuts, foliage > roots > nut > stem; and, for cassava, foliage > roots > stem > tubers. All crops exhibited the lowest concentrations in their edible parts (kernel, nuts, and tubers),

except for the peanut stem, which was slightly lower than the nuts. This finding aligns with studies on rice in China, where the stem and seeds consistently showed the lowest THg concentrations across all measured sites (Yin et al., 2013).

3.3 Tracing uptake and translocation of Hg within crops using Hg stable isotopes

While THg quantifies the extent of overall Hg exposure in the examined crops, we have thus far not been able to fully confirm the Hg uptake pathway or explain translocation processes within the crop. We therefore applied Hg stable isotope analyses to investigate these processes in greater detail. Foliage samples across all crops displayed highly negative MDF values, with δ^{202} Hg values of $-3.83 \pm 0.19\%$ (2 SD) for cassava, $-3.77 \pm 0.19\%$ (2 SD) for peanuts, and $-2.51 \pm 0.32\%$ (1 SD) for maize (Fig. 4). MIF values were all near zero (Δ^{199} Hg range: -0.04 to 0.03% (Fig. 4). Sun et al. (2020) measured similar MDF values in maize foliage ($-2.68 \pm 0.28\%$ (1 SD). Yet they also observed more negative δ^{202} Hg in higher-concentration samples (Sun et al., 2020), which is likely linked to GEM influenced by anthropogenic sources having more negative δ^{202} Hg.

Assuming all the Hg within foliage for these crops grown in unsaturated soils is derived from stomatal assimilation, we can use the mean Hg stable isotope values for GEM (mean MerPAS values from both the PS and Farm1 to provide estimate variance) to estimate the enrichment factors (indicated by ε for MDF and E for MIF) associated with the stomatal assimilation process for the stomatal assimilation process in these crops. We calculate ε^{202} Hg for stomatal assimilation to be -2.60 ± 0.35 , -2.54 ± 0.35 , and $-1.28 \pm 0.43\%$ for cassava, peanuts, and maize, respectively, and these data represent the first time such fractionation factors have been calculated for any agricultural crops. These crop stomatal assimilation MDF enrichment factors fall within the range reported (-1 to -3%) in other vegetation (Zhou et al., 2021; Liu et al., 2021; and references therein). There was a small MIF between GEM and foliage (E^{199} Hg: cassava, -0.05%); peanuts, -0.05%; maize, -0.11%), which is similar to the small range observed during this process elsewhere (Demers et al., 2013). The small negative MIF shift can be attributed

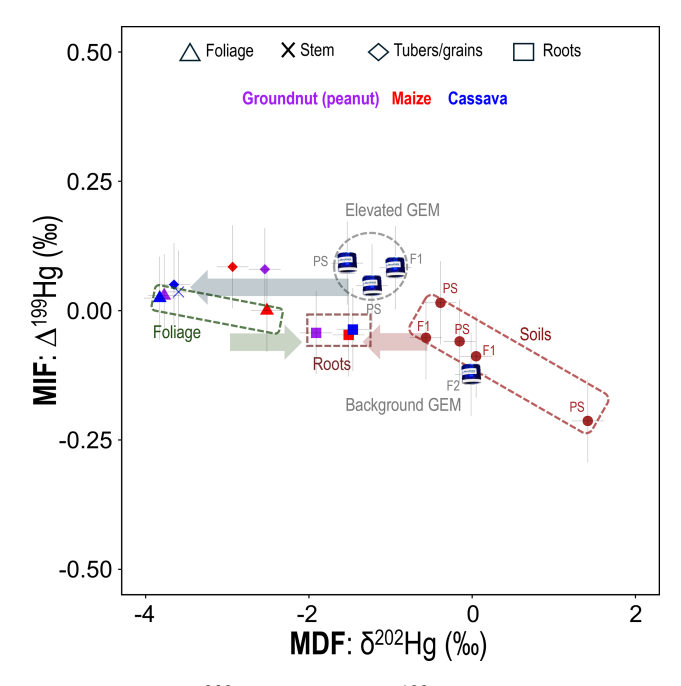


Figure 4. MDF (δ^{202} Hg) and MIF (Δ^{199} Hg) for GEM at the PS, Farm1 (F1), and Farm2 (F2); soil samples at the PS and Farm1 (F1); and crop tissues for Farm1 (F1) only. The direction of the arrows shows approximate MDF from air to foliage (stomatal assimilation; blue arrow), foliage to roots (green arrow), and soil to roots (red arrow). Note that cassava tubers are flesh only (no peel). Full Hg isotope datasets are provided in Sect. S7.

to minor in planta photochemical Hg(II) reduction (Demers et al., 2013) and is typically accompanied by an enrichment in the heavy Hg isotopes and positive shift in δ^{202} Hg; while speculative, this could again be attributable to differing physiological processes (i.e. C₄ photosynthesis).

Crop root samples exhibited negative δ^{202} Hg values (cassava: -1.46%; peanuts: -1.91%; maize: %) that were distinct from both soil and foliage samples, while Δ^{199} Hg values were similar to those of soil and slightly more negative than GEM and foliage samples (Fig. 4). We suggest that the Hg in roots reflects a combination of inputs from both soil and foliage (via stomatal assimilation). Since foliage is a source of energy to plants in the form of the photoassimilates they generate, which are exported to growth (meristems, cambium) and storage (roots, fruits, seeds) tissues via the phloem (Turgeon, 2006), Hg is likely translocated in a similar manner, as has been posited in other studies (Zhou et al., 2021; McLagan et al., 2022a). For maize and peanut roots, the *qualitative* PTD analyses (see Fig. S5) revealed the presence of two distinct Hg pools, which we suggest could be representative of distinct fractions of Hg in (i) the epidermis/cortex (likely derived from surrounding soils) and (ii) inner root tissues: vascular bundle/stele (likely derived from air/foliage).

We also apply a two-endmember mixing model using the mean δ^{202} Hg values of (i) GEM at Farm1 and the PS and (ii) soils at Farm1, minus the MDF of soil to shallow roots (roots above 150 cm) (ε^{202} Hg: -0.35) from Yuan et al. (2022), as endmembers to introduce more quantitative assessment of the Hg uptake mechanisms (air/foliage vs. soil) (Eq. S1). Data reveal that between 47 % (peanuts) and 66 % (cassava) of Hg found in the roots of these crops is derived from air/foliage (Table 1). There is precedence for the transfer of Hg from foliage to roots with a previous study using Hg stable isotopes to indicate 44 %-83 % of Hg in roots is derived from air in selected tree and shrub species (Wang et al., 2020). These data support the hypothesis that the majority of Hg transferred from soil to roots is likely bound to outer root tissue (epidermis/cortex) as suggested elsewhere (Rutter et al., 2011b; Lomonte et al., 2014). Again, root tissue sectioning and analysis for concentrations and stable Hg isotopes would provide the most conclusive evidence of such processes.

Hg stable isotope data for other crop tissues provided further evidence of translocation of Hg away from foliage. Due to the lower concentration and limited available sample, stems could only be analysed for stable isotopes in cassava, and this one sample displayed almost identical MDF and MIF signatures to cassava foliage (93 % derived from air/foliage; Table 1). Edible parts of maize (kernel; 100 % from air/foliage) and cassava (tuber flesh; 95 % from air/foliage) displayed similar patterns (Table 1). Studies on cassava in ASGM regions, such as those by Nyanza et al. (2014), have similarly demonstrated that Hg concentrations in cassava tubers remain low even in highly contaminated soils, emphasizing the influence of foliar pathways. This contrasts with the common assumption that tubers accumulate Hg mainly through soil uptake (Adjorlolo-Gasokpoh et al., 2012).

The only exception to this was peanut nuts, which had a δ^{202} Hg value more similar to roots (39% of nut THg derived from soil) and the most positive Δ^{199} Hg value (0.08 %) of any sample across all studied matrices. While we do not have a clear explanation for the anomalous Δ^{199} Hg value of the nut sample, we link the similar δ^{202} Hg values between peanut roots and nuts to the subsurface growth of the nut. Cassava tubers also grow underground, but their physiological function is as a plant energy storage tissue (Rees et al, 2012) as opposed to the peanut nut, which is a seed used for reproduction (Basuchaudhuri, 2022). The transfer of Hg from soils through peanut shells and into the nut is still somewhat surprising, as other studies have shown the shell to be an effective barrier at preventing metal uptake to the nut (Tang et al., 2024), including for Hg (Namasivayam and Periasamy, 1993; Cobbina et al., 2019). Nonetheless, Liu et al. (2010) observed lower Hg adsorption efficiency by natural (compared to chemically modified) peanut shells, though we note this was in a laboratory study of just shells (nuts removed). Multi-method analyses of peanut shells would be a useful addition to future work.

Table 1. Hg uptake source apportionment in crop tissues using a two-endmember Hg stable isotope mixing model. Foliage is not included, as δ^{202} Hg values for foliage represent one of the source endmembers for each crop. All estimates come with a $\pm 16\%$ uncertainty derived from propagating uncertainty terms through calculations.

	Cassava			Maize		Peanut	
Source	Stem	Tuber flesh	Root	Kernel	Roots	Nut	Roots
Air/foliage Soil/roots	93 % 7 %	95 % 5 %	26 % 74 %		47 % 53 %		41 % 59 %

3.4 Foliage as an important sink of GEM in ASGM areas

We also used Eqs. (S2) and (S3) to assess the annual GEM dry deposition flux from the atmosphere to these crops via stomatal assimilation. The GEM deposition rates from the atmosphere to leaves for peanuts, maize, and cassava were estimated to be 110 ± 80 , 690 ± 130 , and $1170 \pm 180 \,\mathrm{g\,km^{-2}\,yr^{-1}}$, respectively. The relatively high GEM deposition rate observed for cassava shows the higher vulnerability of cassava to Hg uptake despite it being grown once annually. This may be due to its larger biomass compared to maize and peanuts. These data were substantially higher than the $13-25 \,\mathrm{g\,km^{-2}}\,\mathrm{yr^{-1}}$ estimate for soybeans by Casagrande et al. (2020). While this is partly attributable to Casagrande et al. (2020), not accounting for transfer from foliage to other above- or belowground tissues, our estimates were dominated by Hg storage in foliage (90 %-92 % of total; see Table S5.1). Hence, we attribute the differences between the two estimates to differences in distances between ASGM activities and farms/crops, the scale of ASGM operations, and different crop physiological uptake mechanisms. These data provide crucial insight into the role of crop foliage in sequestering atmospheric Hg in regions impacted by ASGM and can be useful in environmental monitoring and risk assessment. In regions with ongoing ASGM activities, these estimates could be used as baselines to monitor shifts in atmospheric Hg concentrations over time. For instance, if emissions from ASGM were to decline due to policy interventions, a corresponding reduction in annual Hg deposition rates would be expected. Conversely, if emissions increase, these crops could serve as bioindicators for heightened atmospheric contamination.

3.5 Human health implications

MeHg concentration data are typically considered the major endpoint for assessing human and environmental health impacts of Hg. MeHg concentrations were consistently below 1% of total Hg (THg) in all samples (Table S7.5), suggesting low methylation rates of Hg(II) in these soils. Moreover, the probable daily intake (PDI) for MeHg in these crops ($< 0.001 \, \mu g \, kg^{-1} \, d^{-1}$), or the sum of their dietary intakes $(0.0010 \pm 0.0016 \, \mu g \, kg^{-1} \, d^{-1})$, is 2 orders of magni-

tude below the USEPA reference dose (RfD) for MeHg of $0.1 \,\mu\text{g kg}^{-1} \,d^{-1}$ (USEPA, 2001). This contrasts data from rice grown in Hg-contaminated areas, which is known to accumulate MeHg (via root uptake) due to the capacity of rice paddies to host anoxic conditions known to produce this highly bioaccumulative species (Zhao et al., 2016, 2020).

While less toxic than MeHg, inorganic Hg has been associated with health effects on gastrointestinal, renal, and nervous systems (Ha et al., 2017; Basu et al., 2023). Due to the low MeHg concentrations, inorganic Hg exposures were assessed using THg concentrations, and these values were adjusted for the lower absorption rates of inorganic Hg (7%; WHO, 1990); this adjustment allows direct comparison of inorganic Hg and THg exposures to the MeHg RfD value (Zhao et al., 2019). While PDI values for inorganic Hg and THg were higher in all edible crop tissues examined (individual crop range: $0.0001 \, \mu g \, kg^{-1} \, d^{-1}$ in maize to $0.016 \,\mu\text{g}\,\text{kg}^{-1}\,\text{d}^{-1}$ in cassava leaves; dietary sum: $0.023 \pm 0.007 \,\mu g \, kg^{-1} \, d^{-1}$; Table S6.1), they are again below the MeHg RfD value. Hence, there is little health risk to the local population from Hg levels ingested during typical consumption of the studied tubers/grains/nuts.

Cassava leaves are commonly consumed in various regions, including Nigeria (El-Sharkawy, 2003); hence, the high inorganic Hg in cassava leaves we observed in particular could pose some risk. Without direct data for estimated dietary intake of cassava leaves in Nigeria, we chose to assume a conservative daily intake rate (50 g d⁻¹; Sect. S6). Latif and Müller (2015), report that cassava leaves are consumed up to $500 \,\mathrm{g}\,\mathrm{d}^{-1}$ in countries such as Zaire and the Democratic Republic of Congo, which is 1 order of magnitude higher than our assumed daily intake rate. Consumption of contaminated cassava leaves at the observed levels of contamination and at rates of 500 g d⁻¹ would surpass RfD levels. Despite the reported health benefits of eating cassava leaves (Latif and Müller, 2015), we suggest dietary caution when consuming cassava foliage grown in close proximity to ASGM, and this likely applies for other edible plant foliage.

Although maize and peanut leaves are not typically consumed by humans, they are frequently used as fodder for livestock (Samkol, 2018; Abdul Rahman et al., 2022). This introduces an additional layer of concern, as the ingestion of Hgladen plants by livestock can lead to the accumulation of Hg in livestock kidneys and liver (Verman et al, 1986; Crout et

al., 2004). Human exposure through the consumption of Hgcontaminated meat and dairy/egg products is an additional understudied potential human exposure pathway. Adding Hg stable isotope analyses to any future work around Hg in livestock in ASGM areas could provide valuable insight into the biogeochemical processes involved.

3.6 Limitations and future work

As noted in Sect. 2.1, the scope of our sampling was limited by the social and geopolitical complexity of the ASGM issue. While it would have been optimal to assess larger crop sampling sizes at each site, we had to respect the wishes of the site operators, the community, and the farmers for whom these crops are their livelihood. Despite the lowerthan-optimal sampling sizes, we achieved robustness through a thorough experimental design that captured samples from all the critical environmental compartments (and different plant tissues) and multi-method analyses. With that, we are confident in our data and the findings made with those data. Future studies should expand upon this work by adding dissected crop tissues (i.e. roots, edible parts) to improve the assessment of uptake pathways, internal cycling of Hg by plants, and translocation into edible tissues. Hg stable isotope analyses should remain a key part of future studies of this nature. Other studies have determined more elevated concentrations of Hg in edible parts of crops near ASGM areas (i.e. Adjorololo-Gasokpoh et al., 2012; Addai-Arhin et al., 2023); hence, if it is feasible, similarly structured studies to our own should attempt to assess ASGM sites of differing (larger) scales and/or the proximity of farms to these sites.

This site was chosen due to existing partnerships that were built through discourse and trust. As described in Moreno-Brush et al. (2020), these partnerships between the communities, miners, local researchers, and international collaborators are critical to the success of Hg biogeochemical assays in ASGM areas. Security and research safety are considerable issues of research conducted in ASGM areas. While this should highlight the need for strong local partnerships, we stress that flexibility and adaption are vital components of such work, which becomes increasingly important as ASGM continues to expand in the Global South.

Code and data availability. No specialized modelling code was used to perform the calculations used in this study, and all data can be recreated from the raw data and equations provided in the Supplement. Please contact the corresponding author for any additional information or questions relating to the data.

Supplement. The Supplement contains all complementary information and all data used within the study, as well as extended details on the study methods. The supplement related to this article is available online at https://doi.org/10.5194/bg-22-5591-2025-supplement.

Author contributions. EOE built research partnerships in Nigeria, contributed to experimental design, led field work and sample collection, undertook sample preparations and analysis, generated figures, and wrote the draft. NV worked on the development of analytical methods (including Hg isotope combust and trap), undertook sample preparation and analysis (including Hg stable isotope analyses in Toulouse), and provided reviews of the article. AOM built connections with the Uke community and mining stakeholders, contributed to experimental design and fieldwork, provided lab space for sample preparations at the University of Lagos, and reviewed the article. NCA built connections with the Uke community and mining stakeholders, contributed to experimental design and fieldwork (including follow-up sampling and MerPAS collections at Farm2), and reviewed the article. JES provided guidance on Hg stable isotope sample extraction methods, led Hg stable isotopes analyses, and provided reviews of the article. SSM undertook all MeHg analyses and provided reviews of the article. DSM conceptualized the study, built research partnerships in Nigeria, worked on the development of analytical methods, contributed to figures, provided draft guidance, and reviewed the article.

Competing interests. At least one of the (co-)authors is a member of the editorial board of *Biogeosciences*. The peer-review process was guided by an independent editor, and the authors also have no other competing interests to declare.

Disclaimer. Publisher's note: Copernicus Publications remains neutral with regard to jurisdictional claims made in the text, published maps, institutional affiliations, or any other geographical representation in this paper. While Copernicus Publications makes every effort to include appropriate place names, the final responsibility lies with the authors.

Acknowledgements. We thank the support from Zinariya Kyautar Allah (Mining) Venture Ltd. and the community of Uke, Nigeria, for welcoming us into their community and being active and willing contributors to this work. We acknowledge contributions of the Analytical Services Unit (ASU) team at Queen's University (Meesha Thompson, Paula Whitely, Dale Marecak, and Graham Cairns) for their support and feedback on Hg analyses. We thank Jason Demers and Bridget Bergquist for their direction and guidance in setting up our lab for Hg stable isotope sample preparations and extractions. We also thank D. K. Olukoya Central Research and Reference Laboratories from the University of Lagos for providing support with sample-drying in Nigeria. We acknowledge Carl Mitchell for providing the use of MeHg analysis methods to assess MeHg concentrations in plant and soil samples. Jerome Chmeleff is thanked for assistance with Hg isotope analyses. Finally, we thank the three reviewers and associate editor for their contributions in bringing this work to publication.

Financial support. We received an internal, alumni-based graduate scholarship/award (Maria Nathanson/IAMGOLD Fund: 50540) from Queen's University for this work.

Review statement. This paper was edited by Johannes Bieser and reviewed by Jan Gacnik and two anonymous referees.

References

- Abdul Rahman, N., Larbi, A., Addah, W., Sulleyman, K. W., Adda, J. K., Kizito, F., and Hoeschle-Zeledon, I.: Optimizing food and feed in maize—livestock systems in northern Ghana: The effect of maize leaf stripping on grain yield and leaf fodder quality, Agriculture, 12, 275, https://doi.org/10.3390/agriculture12020275, 2022.
- Achina-Obeng, R. and Aram, S. A.: Informal artisanal and small-scale gold mining (ASGM) in Ghana: Assessing environmental impacts, reasons for engagement, and mitigation strategies, Resour. Policy, 78, 102907, https://doi.org/10.1016/j.resourpol.2022.102907, 2022.
- Addai-Arhin, S., Novirsa, R., Jeong, H., Phan, Q. D., Hirota, N., Ishibashi, Y., Shiratsuchi, H., and Arizono, K.: Mercury waste from artisanal and small-scale gold mining facilities: a risk to farm ecosystems a case study of Obuasi, Ghana, Environ. Sci. Pollut. R., 30, 4293–4308, https://doi.org/10.1007/s11356-022-22456-4, 2023.
- Adjorlolo-Gasokpoh, A., Golow, A. A., and Kambo-Dorsa, J.: Mercury in the surface soil and cassava, Manihot esculenta (flesh, leaves, and peel) near goldmines at Bogoso and Prestea, Ghana, B. Environ. Contam. Tox., 89, 1106–1110, https://doi.org/10.1007/s00128-012-0849-7, 2012.
- Ariya, P. A., Amyot, M., Dastoor, A., Deeds, D., Feinberg, A., Kos, G., Poulain, A., Ryjkov, A., Semeniuk, K., Subir, M., and Toyota, K.: Mercury physicochemical and biogeochemical transformation in the atmosphere and at atmospheric interfaces: a review and future directions, Chem. Rev., 115, 3760–3802, https://doi.org/10.1021/cr500667e, 2015.
- Assad. M., Parelle. J., Cazaux. D., Gimbert. F., Chalot, M., and Tatin-Froux, F.: Mercury up-1-7, take into poplar leaves, Chemosphere, 146, https://doi.org/10.1016/j.chemosphere.2015.11.103, 2016.
- Basu, N., Bastiansz, A., Dórea, J. G., Fujimura, M., Horvat, M., Shroff, E., Weihe, P., and Zastenskaya, I.: Our evolved understanding of the human health risks of mercury, Ambio, 52, 877–896, https://doi.org/10.1007/s13280-023-01831-6, 2023.
- Basuchaudhuri, P.: Physiology of the Peanut Plant, CRC Press, Boca Raton, USA, p. 430, https://doi.org/10.1201/9781003262220, 2022.
- Beauford, W., Barber, J., and Barringer, A. R.: Uptake and distribution of mercury within higher plants. Physiologia Plantarum, 39, 261–265, https://doi.org/10.1111/j.1399-3054.1977.tb01880.x, 1977.
- Bergquist, B. A. and Blum, J. D.: The odds and evens of mercury isotopes: applications of mass-dependent and mass-independent isotope fractionation, Elements, 5, 353–357, https://doi.org/10.2113/gselements.5.6.353, 2009.
- Biester, H. and Scholz, C.: Determination of mercury binding forms in contaminated soils: mercury pyrolysis versus sequential extractions, Environ. Sci. Technol., 31, 233–239, https://doi.org/10.1021/es960369h, 1996.

- Blum, J. D. and Bergquist, B. A.: Reporting of variations in the natural isotopic composition of mercury, Anal. Bioanal. Chem., 388, 353–359, https://doi.org/10.1007/s00216-007-1236-9, 2007.
- Bose-O'Reilly, S., Drasch, G., Beinhoff, C., Rodrigues-Filho, S., Roider, G., Lettmeier, B., Maydl, A., Maydl, S., and Siebert, U.: Health assessment of artisanal gold miners in Indonesia, Sci. Total Environ., 408, 713–725, https://doi.org/10.1016/j.scitotenv.2009.10.070, 2010.
- Bräutigam, A. and Gowik, U.: Photorespiration connects C₃ and C₄ photosynthesis, J. Exp. Bot., 67, 2953–2962, https://doi.org/10.1093/jxb/erw056, 2016.
- Browne, C. L. and Fang, S. C.: Differential uptake of mercury vapor by gramineous C₃ and C₄ plants, Plant Physiol., 72, 1040–1042, https://doi.org/10.1104/pp.72.4.1040, 1983.
- Bugmann, A., Brugger, F., Zongo, T., and Van der Merwe, A.: "Doing ASGM without mercury is like trying to make omelets without eggs": Understanding the persistence of mercury use among artisanal gold miners in Burkina Faso, Environ. Sci. Policy, 133, 87–97, https://doi.org/10.1016/j.envsci.2022.03.009, 2022.
- Casagrande, G. C. R., Franco, D. N. D. M., Moreno, M. I. C., de Andrade, E. A., Battirola, L. D., and de Andrade, R. L. T.: Assessment of atmospheric mercury deposition in the vicinity of artisanal and small-scale gold mines using Glycine max as bioindicators, Water Air Soil Poll., 231, 1–14, https://doi.org/10.1007/s11270-020-04918-y, 2020.
- Cheng, Y., Nakajima, K., Nansai, K., Seccatore, J., Veiga, M. M., and Takaoka, M.: Examining the inconsistency of mercury flow in post-Minamata Convention global trade concerning artisanal and small-scale gold mining activity. Resour. Conserv. Recycl., 185, 106461, https://doi.org/10.1016/j.resconrec.2022.106461, 2022.
- Cobbina, S. J., Duwiejuah, A. B., and Quainoo, A. K.: Single and 90 simultaneous adsorption of heavy metals onto groundnut shell biochar produced under fast and slow pyrolysis, Int. J. Environ. Sci. Te., 16, 3081–3090, https://doi.org/10.1007/s13762-018-1910-9, 2019.
- Crout, N. M. J., Beresford, N. A., Dawson, J. M., Soar, J., and Mayes, R. W.: The transfer of ⁷³As, ¹⁰⁹Cd and ²⁰³Hg to the milk and tissues of dairy cattle, J. Agr. Sci., 142, 203–212, https://doi.org/10.1017/S0021859604004186, 2004.
- Demers, J. D., Blum, J. D., and Zak, D. R.: Mercury isotopes in a forested ecosystem: Implications for air-surface exchange dynamics and the global mercury cycle, Global Biogeochem. Cy., 27, 222–238, https://doi.org/10.1002/gbc.20021, 2013.
- El-Sharkawy, M. A.: Cassava biology and physiology, Plant Mol. Biol., 53, 621–641, https://doi.org/10.1023/B:PLAN.0000019109.01740.c6, 2003.
- El-Sharkawy, M. A. and Cock, J. H.: C₃-C₄ intermediate photosynthetic characteristics of cassava (Manihot esculenta Crantz) I. Gas exchange, Photosynth. Res., 12, 219–235, https://doi.org/10.1007/BF00055122, 1987.
- Enrico, M., Balcom, P., Johnston, D. T., Foriel, J., and Sunderland, E. M.: Simultaneous combustion preparation for mercury isotope analysis and detection of total mercury using a direct mercury analyzer, Anal. Chim. Acta, 1154, 338327, https://doi.org/10.1016/j.aca.2021.338327, 2021.
- Essumang, D. K., Dodoo, D. K., Obiri, S., and Yaney, J. Y.: Arsenic, cadmium, and mercury in cocoyam (Xanthosoma sagititolium) and watercocoyam (Colocasia esculenta) in Tarkwa a

- mining community, Bull. Environ. Contam. Toxicol., 79, 377–379, https://doi.org/10.1007/s00128-007-9244-1, 2007.
- Fu, X., Zhu, W., Zhang, H., Sommar, J., Yu, B., Yang, X., Wang, X., Lin, C.-J., and Feng, X.: Depletion of atmospheric gaseous elemental mercury by plant uptake at Mt. Changbai, Northeast China, Atmos. Chem. Phys., 16, 12861–12873, https://doi.org/10.5194/acp-16-12861-2016, 2016.
- Fu, X., Liu, C., Zhang, H., Xu, Y., Zhang, H., Li, J., Lyu, X., Zhang, G., Guo, H., Wang, X., Zhang, L., and Feng, X.: Isotopic compositions of atmospheric total gaseous mercury in 10 Chinese cities and implications for land surface emissions, Atmos. Chem. Phys., 21, 6721–6734, https://doi.org/10.5194/acp-21-6721-2021, 2021.
- Gerson, J. R., Szponar, N., Zambrano, A. A., Bergquist, B., Broadbent, E., Driscoll, C. T., Erkenswick, G., Evers, D. C., Fernandez, L. E., Hsu-Kim, H., Inga, G., Lansdale, K. N., Marchese, M. J., Martinez, A., Moore, C., Pan, W. K., Purizaca, R. P., Sánchez, V., Silman, M., Ury, E. A., Vega, C., Watsa, M., and Bernhardt, E. S.: Amazon forests capture high levels of atmospheric mercury pollution from artisanal gold mining, Nat. Commun., 13, https://doi.org/10.1038/s41467-022-27997-3, 2022.
- Glauser, E., Wohlgemuth, L., Conen, F., and Jiskra, M.: Total mercury accumulation in aboveground parts of maize plants (Zea mays) throughout a growing season, J. Plant Interact., 17, 239–243, https://doi.org/10.1080/17429145.2022.2028914, 2022.
- Golow, A. A., and Adzei, E.A.: Mercury in surface soil and cassava crop near an alluvial goldmine at Dunkwa-on-Offin, Ghana, Bull. Environ. Contam. Toxicol., 69, 228–235, https://doi.org/10.1007/s00128-002-0051-4, 2002.
- González-Carrasco, V., Velasquez-Lopez, P. C., Olivero-Verbel, J., and Pájaro-Castro, N.: Air mercury contamination in the gold mining town of Portovelo, Ecuador, B. Environ. Contam. Tox., 87, 250–253, https://doi.org/10.1007/s00128-011-0345-5, 2011.
- Grigg, A. R., Kretzschmar, R., Gilli, R. S., and Wiederhold, J. G.: Mercury isotope signatures of digests and sequential extracts from industrially contaminated soils and sediments, Sci. Total Environ., 636, 1344–1354, https://doi.org/10.1016/j.scitotenv.2018.04.261, 2018.
- Ha, E., Basu, N., Bose-O'Reilly, S., Dórea, J. G., McSorley, E., Sakamoto, M., and Chan, H. M.: Current progress on understanding the impact of Mercury on human health, Environ. Res., 152, 419–433, https://doi.org/10.1016/j.envres.2016.06.042, 2017.
- Hentschel, T., Hruschka, F., and Priester, M.: Global report on artisanal and small-scale mining, Mining, minerals and sustainable development, International Institute for Environment and Development, London, UK, No. 70, https://intranetua.uantof.cl/crea/cguerra/pdffiles/otros/070_globalasm.pdf (last access: 06 October 2025), 2002.
- Hinton, J., Veiga, M. M., and Veiga, A.: Clean artisanal gold mining: a utopian approach?, J. Clean. Prod., 11, 99–115, https://doi.org/10.1016/s0959-6526(02)00031-8, 2003.
- Iorhemba, A., and Mijinyawa, Y.: Development of Wind Rosettes for Farmstead Planning and Layout in North Central Nigeria, Int. J. Adv. Eng. Manag., 3, 671–679, https://ijaem.net/issue_dcp/Development%20of%20Wind%20Rosettes%20for%20Farmstead%20Planning%20and%20Layout%20in%20North%20Central%20Nigeria.pdf (last access: 6 October 2025), 2021

- Jiskra, M., Wiederhold, J. G., Skyllberg, U., Kronberg, R. M., Hajdas, I., and Kretzschmar, R.: Mercury deposition and reemission pathways in boreal forest soils investigated with Hg isotope signatures, Environ. Sci. Technol., 49, 7188–7196, https://doi.org/10.1021/acs.est.5b00742, 2015.
- Jiskra, M., Sonke, J. E., Obrist, D., Bieser, J., Ebinghaus, R., Myhre, C. L., Pfaffhuber, K. A., Wängberg, I., Kyllönen, K., Worthy, D., Martin, L. G., Labuschagne, C., Mkololo, T., Ramonet, M., Magand, O., and Dommergue, A.: A vegetation control on seasonal variations in global atmospheric mercury concentrations, Nat. Geosci., 11, 244–250, https://doi.org/10.1038/s41561-018-0078-8, 2018.
- Jiskra, M., Heimbürger-Boavida, L. E., Desgranges, M. M., Petrova, M. V., Dufour, A., Ferreira-Araujo, B., Masbou, J., Chmeleff, J., Thyssen, M., Point, D., and Sonke, J. E.: Mercury stable isotopes constrain atmospheric sources to the ocean, Nature, 597=, 678–682, https://doi.org/10.1038/s41586-021-03859-8, 2021.
- Jønsson, J. B., Charles, E., and Kalvig, P.: Toxic mercury versus appropriate technology: Artisanal gold miners' retort aversion, Resour. Policy, 38, 60–67, https://doi.org/10.1016/j.resourpol.2012.09.001, 2013.
- Kawakami, T., Konishi, M., Imai, Y., and Soe, P. S.: Diffusion of mercury from artisanal small-scale gold mining (ASGM) sites in Myanmar, GEOMATE J., 17, 228–235, https://doi.org/10.21660/2019.61.4823, 2019.
- Laacouri, A., Nater, E. A., and Kolka, R. K.: Distribution and uptake dynamics of mercury in leaves of common deciduous tree species in Minnesota, USA, Environ. Sci. Technol., 47, 10462–10470, https://doi.org/10.1021/es401357z, 2013.
- Latif, S. and Müller, J.: Potential of cassava leaves in human nutrition: A review, Trends Food Sci. Tech., 44, 147–158, https://doi.org/10.1016/j.tifs.2015.04.006, 2015.
- Lewis, D., McNeill, R., and Shabalala, Z.: Gold worth billions smuggled out of Africa, Reuters, https://www.reuters.com/ article/us-gold-africa-smuggling-exclusive-idUSKCN1S00V4 (last access: 11 November 2023), 2019.
- Liu, Y., Lin, C. J., Yuan, W., Lu, Z., and Feng, X.: Translocation and distribution of mercury in biomasses from subtropical forest ecosystems: Evidence from stable mercury isotopes, Acta Geochim., 40, 42–50, https://doi.org/10.1007/s11631-020-00441-3, 2021.
- Liu, Y., Sun, X., and Li, B.: Adsorption of Hg²⁺ and Cd²⁺ by ethylenediamine modified peanut shells, Carbohydr. Polym., 81, 335–339, https://doi.org/10.1016/j.carbpol.2010.02.020, 2010.
- Lomonte, C., Wang, Y., Doronila, A., Gregory, D., Baker, A. J., Siegele, R., and Kolev, S. D.: Study of the spatial distribution of mercury in roots of vetiver grass (Chrysopogon zizanioides) by micro-PIXE spectrometry, Int. J. Phytoremediat., 16, 1170– 1182, https://doi.org/10.1080/15226514.2013.821453, 2014.
- Mao, Y., Li, Y., Richards, J., and Cai, Y.: Investigating uptake and translocation of mercury species by sawgrass (Cladium jamaicense) using a stable isotope tracer technique, Environ. Sci. Technol., 47, 9678–9684, https://doi.org/10.1021/es400546s, 2013.
- Marshall, B., Camacho, A. A., Jimenez, G., and Veiga, M. M.: Mercury challenges in Mexico: regulatory, trade and environmental impacts, Atmosphere, 12, 57, https://doi.org/10.3390/atmos12010057, 2020.

- Mashyanov, N. R., Pogarev, S. E., Panova, E. G., Panichev, N., and Ryzhov, V.: Determination of mercury thermospecies in coal, Fuel, 203, 973–980, https://doi.org/10.1016/j.fuel.2017.03.085, 2017.
- McLagan, D. S., Mitchell, C. P., Huang, H., Lei, Y. D., Cole, A. S., Steffen, A., Hung, H., and Wania, F.: A high-precision passive air sampler for gaseous mercury, Environ. Sci. Tech. Let., 3, 24–29, https://doi.org/10.1021/acs.estlett.5b00319, 2016.
- McLagan, D. S., Monaci, F., Huang, H., Lei, Y. D., Mitchell, C. P., and Wania, F.: Characterization and quantification of atmospheric mercury sources using passive air samplers, J. Geophys. Res.-Atmos., 124, 2351–2362, https://doi.org/10.1029/2018JD029373, 2019.
- McLagan, D. S., Biester, H., Navrátil, T., Kraemer, S. M., and Schwab, L.: Internal tree cycling and atmospheric archiving of mercury: examination with concentration and stable isotope analyses, Biogeosciences, 19, 4415–4429, https://doi.org/10.5194/bg-19-4415-2022, 2022a.
- McLagan, D. S., Schwab, L., Wiederhold, J. G., Chen, L., Pietrucha, J., Kraemer, S. M., and Biester, H.: Demystifying mercury geochemistry in contaminated soil–groundwater systems with complementary mercury stable isotope, concentration, and speciation analyses, Environ. Sci.-Proc. Imp., 24, 1406–1429, https://doi.org/10.1039/D1EM00368B, 2022b.
- Millhollen, A. G., Gustin, M. S., and Obrist, D.: Foliar mercury accumulation and exchange for three tree species, Environ. Sci. Technol., 40, 6001–6006, https://doi.org/10.1021/es0609194, 2006.
- Mitchell, C. P. and Gilmour, C. C.: Methylmercury production in a Chesapeake Bay salt marsh, J. Geophys. Res.-Biogeosci., 113, https://doi.org/10.1029/2008JG000765, 2008.
- Moreno-Brush, M., McLagan, D. S., and Biester, H.: Fate of mercury from artisanal and small-scale gold mining in tropical rivers: Hydrological and biogeochemical controls. A critical review, Crit. Rev. Environ. Sci. Technol., 50, 437–475, https://doi.org/10.1080/10643389.2019.1629793, 2020.
- Munthe, J., Kindbom, K., Parsmo, R., and Yaramenka, K.: Technical Background Report to the Global Mercury Assessment 2018, United Nations Environ-Programme (UNEP), https://www. mental Kenya, unep.org/globalmercurypartnership/resources/report/ technical-background-report-global-mercury-assessment-2018 (last access: 24 June 2024), 2019.
- Nakazawa, K., Nagafuchi, O., Kawakami, T., Inoue, T., Elvince, R., Kanefuji, K., Nur, I., Napitupulu, M., Basir-Cyio, M., Kinoshita, H., and Shinozuka, K.: Human health risk assessment of atmospheric mercury inhalation around three artisanal smallscale gold mining areas in Indonesia, Environ. Sci. Atmos., 1, 423–433, https://doi.org/10.1039/D0EA00019A, 2021.
- Namasivayam, C. and Periasamy, K.: Bicarbonate-treated peanut hull carbon for mercury (II) removal from aqueous solution, Water Res., 27, 1663–1668, https://doi.org/10.1016/0043-1354(93)90130-A, 1993.
- Niu, Z., Zhang, X., Wang, Z., and Ci, Z.: Field controlled experiments of mercury accumulation in crops from air and soil, Environ. Pollut., 159, 2684–2689, https://doi.org/10.1016/j.envpol.2011.05.029, 2011.
- Nyanza, E. C., Dewey, D., Thomas, D. S., Davey, M., and Ngallaba, S. E.: Spatial distribution of mercury and arsenic levels in

- water, soil and cassava plants in a community with long history of gold mining in Tanzania, B. Environ. Contam. Tox., 93, 716–721, https://doi.org/10.1007/s00128-014-1315-5, 2014.
- Obrist, D., Agnan, Y., Jiskra, M., Olson, C. L., Colegrove, D. P., Hueber, J., Moore, C. W., Sonke, J. E., and Helmig, D.: Tundra uptake of atmospheric elemental mercury drives Arctic mercury pollution, Nature, 547, 201–204, https://doi.org/10.1038/nature22997, 2017.
- Obrist, D., Roy, E. M., Harrison, J. L., Kwong, C. F., Munger, J. W., Moosmüller, H., Romero, C. D., Sun, S., Zhou, J., and Commane, R.: Previously unaccounted atmospheric mercury deposition in a midlatitude deciduous forest, P. Natl. Acad. Sci. USA, 118, e2105477118, https://doi.org/10.1073/pnas.2105477118, 2021.
- Odukoya, A. M., Uruowhe, B., Watts, M. J., Hamilton, E. M., Marriott, A. L., Alo, B., and Anene, N. C.: Assessment of bioaccessibility and health risk of mercury within soil of artisanal gold mine sites, Niger, North-central part of Nigeria, Environ. Geochem. Hlth., 44, 893–909, https://doi.org/10.1007/s10653-021-00991-2, 2022.
- PlanetGOLD: Global Forum Artisanal & Smallon Scale Gold Mining, PlanetGOLD Project, UNEP. Nairobi, https://www.planetgold.org/ Kenya, 852022-global-forum-artisanal-small-scale-gold-mining, (last access: 21 October 2024), 2022.
- Qiu, G., Feng, X., Li, P., Wang, S., Li, G., Shang, L., and Fu, X.: Methylmercury accumulation in rice (*Oryza sativa* L.) grown at abandoned mercury mines in Guizhou, China, J. Agr. Food Chem., 56, 2465–2468, https://doi.org/10.1021/jf073391a, 2008.
- Rea, A. W., Lindberg, S. E., and Keeler, G. J.: Assessment of dry deposition and foliar leaching of mercury and selected trace elements based on washed foliar and surrogate surfaces, Environ. Sci. Technol., 34, 2418–2425, https://doi.org/10.1021/es991305k, 2000.
- Rees, D., Westby, A., Tomlins, K., Van Oirschot, Q., Cheema, M. U., Cornelius, E., and Amjad, M.: Tropical root crops, in: Crop Post-Harvest: Science and Technology: Perishables, edited by: Rees, D., Farrell, G., and Orchard, J., Wiley-Blackwell Publishing, Susse, UK, 392–413, https://doi.org/10.1002/9781444354652.ch18, 2012.
- Rose, C. H., Ghosh, S., Blum, J. D., and Bergquist, B. A.: Effects of ultraviolet radiation on mercury isotope fractionation during photo-reduction for inorganic and organic mercury species, Chem. Geol., 405, 102–111, https://doi.org/10.1016/j.chemgeo.2015.02.025, 2015.
- Rutter, A. P., Schauer, J. J., Shafer, M. M., Creswell, J. E., Olson, M. R., Robinson, M., Collins, R. M., Parman, A. M., Katzman, T. L., and Mallek, J. L.: Dry deposition of gaseous elemental mercury to plants and soils using mercury stable isotopes in a controlled environment, Atmos. Environ., 45, 848–855, https://doi.org/10.1016/j.atmosenv.2010.11.025, 2011a.
- Rutter, A. P., Schauer, J. J., Shafer, M. M., Creswell, J., Olson, M. R., Clary, A., Robinson, M., Parman, A. M., and Katzman, T. L.: Climate sensitivity of gaseous elemental mercury dry deposition to plants: Impacts of temperature, light intensity, and plant species, Environ. Sci. Technol., 45, 569–575, https://doi.org/10.1021/es102687b, 2011b.
- Samkol, P.: Groundnut foliage as feed for Cambodian cattle, PhD thesis, Acta Univ. Agric. Sueciae, 201, 1–50, https://core.ac.uk/

- download/pdf/211564208.pdf (last access: 21 December 2024), 2018
- Seccatore, J., Veiga, M., Origliasso, C., Marin, T., and De Tomi, G.: An estimation of the artisanal small-scale production of gold in the world, Sci. Total Environ., 496, 662–667, https://doi.org/10.1016/j.scitotenv.2014.05.003, 2014.
- Si, M., McLagan, D. S., Mazot, A., Szponar, N., Bergquist, B., Lei, Y. D., Mitchell, C. P. J., and Wania, F.: Measurement of atmospheric mercury over volcanic and fumarolic regions on the North Island of New Zealand using passive air samplers, ACS Earth Space Chem., 4, 2435–2443, https://doi.org/10.1021/acsearthspacechem.0c00274, 2020.
- Snow, M. A., Darko, G., Gyamfi, O., Ansah, E., Breivik, K., Hoang, C., Lei, Y. D., and Wania, F.: Characterization of inhalation exposure to gaseous elemental mercury during artisanal gold mining and e-waste recycling through combined stationary and personal passive sampling, Environ. Sci.-Proc. Imp., 23, 569–579, https://doi.org/10.1039/d0em00494d, 2021.
- Sonke, J. E., Schäfer, J., Chmeleff, J., Audry, S., Blanc, G., and Dupré, B.: Sedimentary mercury stable isotope records of atmospheric and riverine pollution from two major European heavy metal refineries, Chem. Geol., 279, 90–100, https://doi.org/10.1016/j.chemgeo.2010.09.017, 2010.
- Sprovieri, F., Pirrone, N., Bencardino, M., D'Amore, F., Carbone, F., Cinnirella, S., Mannarino, V., Landis, M., Ebinghaus, R., Weigelt, A., Brunke, E.-G., Labuschagne, C., Martin, L., Munthe, J., Wängberg, I., Artaxo, P., Morais, F., Barbosa, H. D. M. J., Brito, J., Cairns, W., Barbante, C., Diéguez, M. D. C., Garcia, P. E., Dommergue, A., Angot, H., Magand, O., Skov, H., Horvat, M., Kotnik, J., Read, K. A., Neves, L. M., Gawlik, B. M., Sena, F., Mashyanov, N., Obolkin, V., Wip, D., Feng, X. B., Zhang, H., Fu, X., Ramachandran, R., Cossa, D., Knoery, J., Marusczak, N., Nerentorp, M., and Norstrom, C.: Atmospheric mercury concentrations observed at ground-based monitoring sites globally distributed in the framework of the GMOS network, Atmos. Chem. Phys., 16, 11915–11935, https://doi.org/10.5194/acp-16-11915-2016, 2016.
- Streets, D. G., Horowitz, H. M., Lü, Z., Levin, L., Thackray, C. P., and Sunderland, E. M.: Global and regional trends in mercury emissions and concentrations, 2010–2015, Atmos. Environ., 201, 417–427, https://doi.org/10.1016/j.atmosenv.2018.12.031, 2019.
- Suhadi, S., Sueb, S., Muliya, B. K., and Ashoffi, A. M.: Pollution of mercury and cyanide in soils and plants surrounding the Artisanal and Small-Scale Gold Mining (ASGM) at Sekotong District, West Lombok, West Nusa Tenggara, Biol. Environ. Pollut., 1, 30–37, https://doi.org/10.31763/bioenvipo.v1i1.392, 2021.
- Sun, R., Enrico, M., Heimbürger, L. E., Scott, C., and Sonke J. E.: A double-stage tube furnace—acid-trapping protocol for the pre-concentration of mercury from solid samples for isotopic analysis, Anal. Bioanal. Chem., 405, 6771–6781, https://doi.org/10.1007/s00216-013-7152-2, 2013.
- Sun, G., Feng, X., Yin, R., Zhao, H., Zhang, L., Sommar, J., Li, Z., and Zhang, H.: Corn (*Zea mays* L.): A low methylmercury staple cereal source and an important biospheric sink of atmospheric mercury, and health risk assessment, Environ. Int., 131, 104971, https://doi.org/10.1016/j.envint.2019.104971, 2019.
- Sun, T., Wang, Z., Zhang, X., Niu, Z., and Chen, J.: Influences of high-level atmospheric gaseous elemental mercury on methylmercury accumulation in

- maize (*Zea mays* L.), Environ. Pollut., 265, 114890, https://doi.org/10.1016/j.envpol.2020.114890, 2020.
- Szponar, N., McLagan, D. S., Kaplan, R. J., Mitchell, C. P. J., Wania, F., Steffen, A., Stupple, G. W., Monaci, F., and Bergquist, B. A.: Isotopic characterization of atmospheric gaseous elemental mercury by passive air sampling, Environ. Sci. Technol., 54, 10533–10543, https://doi.org/10.1021/acs.est.0c02251, 2020.
- Szponar, N., Vega, C. M., Gerson, J. R., McLagan, D. S., Pillaca, M., Antoni, S., Lee, D., Rahman, N., Fernandez, L., Bernhardt, E., Kiefer, A., Mitchell, C. P. J., Wania, F., and Bergquist, B.: Tracing atmospheric mercury from artisanal and small-scale gold mining, Environ. Sci. Technol., 59, 5021–5033, https://doi.org/10.1021/acs.est.4c10521, 2025.
- Tang, X., Wang, Y., Ding, C., Yin, Y., Zhou, Z., Zhang, T., and Wang, X.: Cadmium found in peanut (*Arachis hypogaea* L.) kernels mainly originates from root uptake rather than shell absorption from soil, Pedosphere, 34, 726–735, https://doi.org/10.1016/j.pedsph.2023.05.009, 2024.
- Telmer, K. H. and Veiga, M. M.: World emissions of mercury from artisanal and small-scale gold mining, in: Mercury Fate and Transport in the Global Atmosphere: Emissions, Measurements and Models, Springer, Boston, USA, 131–172, https://doi.org/10.1007/978-0-387-93958-2 6, 2009.
- Turgeon, R.: Phloem loading: how leaves gain their independence, BioScience, 56, 15–24, https://doi.org/10.1641/0006-3568(2006)056[0015:PLHLGT]2.0.CO;2, 2006.
- UNEP: Minamata Convention on Mercury, United Nations Environmental Programme, Kenya, NGA, https://www.unep.org/resources/report/minamata-convention-mercury (last access: 24 June 2024), 2013.
- USEPA: Integrated Risk Information System. Methylmercury (MeHg) (CASRN 22967-92-6), US Environmental Protection Agency, Washington, DC, USA, https://cfpub.epa.gov/ncea/iris/iris_documents/documents/subst/0073_summary.pdf (last access: 17 March 2024), 2001.
- USEPA: Method 7473: Mercury in solids and Solutions by Thermal Decomposition, Amalgamation, and Atomic Absorption Spectro-Photometry. Test methods for evaluating solid wastes. Physical/Chemical Methods. SW-846 On-Line, United States Environmental Protection Agency (UNEP), Washington, DC, USA, https://www.epa.gov/sites/default/files/2015-12/documents/7473.pdf (last access: 6 October 2025), 2007.
- USEPA: Operating Procedure: Soil Sampling, US Environmental Protection Agency (USEPA), Washington, DC, USA, https://www.epa.gov/sites/production/files/2015-06/documents/Soil-Sampling.pdf (last access: 6 October 2025), 2023.
- Vaňková, M., Vieira, A. M. D., Ettler, V., Vaněk, A., Trubač, J., Penížek, V., and Mihaljevič, M.: Tracing anthropogenic mercury in soils from Fe–Hg mining/smelting area: Isotopic and speciation insights, Chemosphere, 357, 142038, https://doi.org/10.1016/j.chemosphere.2024.142038, 2024.
- Veiga, M. M., Maxson, P. A., and Hylander, L. D.: Origin and consumption of mercury in small-scale gold mining, J. Clean. Prod., 14, 436–447, https://doi.org/10.1016/j.jclepro.2004.08.010, 2006.
- Verbrugge, B. and Geenen, S.: The gold commodity frontier: A fresh perspective on change and diversity in the global gold mining economy, Extr. Ind. Soc., 6, 413–423, https://doi.org/10.1016/j.exis.2018.10.014, 2019.

- Verité Inc.: The Nexus of Illegal Gold Mining and Human Trafficking in Global Supply Chains. Lessons from Latin America, Verité Inc. on behalf of Global Initiative Against Transnational Organized Crime, Northampton, USA, https://globalinitiative.net/wp-content/uploads/2018/01/The-nexus-of-illegal-gold-mining.pdf (last access: 06 October 2025), 2016.
- Wang, D., Li, Z., and Wang, Q.: Ecological restoration reduces mercury in corn kernel and the distinction of mercury in corn plants in rural China A case in Wuchuan mercury mining area, Ecotox. Environ. Safe., 271, 115964, https://doi.org/10.1016/j.ecoenv.2024.115964, 2024.
- Wang, X., Yuan, W., Lin, C., Luo, J., Wang, F., Feng, X., Fu, X., and Liu, C.: Underestimated sink of atmospheric mercury in a deglaciated forest chronosequence, Environ. Sci. Technol., 54, 8083–8093, https://doi.org/10.1021/acs.est.0c01667, 2020.
- Weinhouse, C., Gallis, J. A., Ortiz, E., Berky, A. J., Morales, A. M., Diringer, S. E., Harrington, J., Bullins, P., Rogers, L., Hare-Grogg, J., Hsu-Kim, H., and Pan, W. K.: A population-based mercury exposure assessment near an artisanal and small-scale gold mining site in the Peruvian Amazon, J. Expo. Sci. Env. Epid., 31, 126–136, https://doi.org/10.1038/s41370-020-0234-2, 2021.
- WHO: Environmental health criteria 101: Methylmercury, World Health Organization, Geneva, CHE, https://apps.who.int/iris/bitstream/handle/10665/38082/9241571012_eng.pdf (last access: 6 October 2025), 1990.
- World Gold Council: Gold mine production, World Gold Council, London, UK, https://www.gold.org/goldhub/data/ historical-mine-production (last access: 6 October 2025), 2024.
- Xia, Z., Du, Z., Zhou, X., Jiang, S., Zhu, T., Wang, L., Chen, F., Carvalho, L., Zou, M., López-Lavalle, L. a. B., Zhang, X., Xu, L., Wang, Z., Chen, M., Feng, B., Wang, S., Li, M., Li, Y., Wang, H., Liu, S., Bao, Y., Zhao, L., Zhang, C., Xiao, J., Guo, F., Shen, X., Lu, C., Qiao, F., Ceballos, H., Yan, H., Zhang, H., He, S., Zhao, W., Wan, Y., Chen, Y., Huang, D., Li, K., Liu, B., Peng, M., Zhang, W., Muller, B., Chen, X., Luo, M.C., Xiao, J., and Wang, W.: Pan-genome and Haplotype Map of Cultivars and Their Wild Ancestors Provides Insights into Selective Evolution of Cassava (Manihot esculentaCrantz), bioRxiv, https://doi.org/10.1101/2023.07.02.546475, 2023.

- Yin, R., Feng, X., and Meng, B.: Stable mercury isotope variation in rice plants (*Oryza sativa* L.) from the Wanshan mercury mining district, SW China, Environ. Sci. Technol., 47, 2238–2245, https://doi.org/10.1021/es304302a, 2013.
- Yoshimura, A., Koyo, S., and Veiga, M. M.: Estimation of mercury losses and gold production by Artisanal and Small-Scale Gold Mining (ASGM), J. Sustain. Met., 7, 1045–1059, https://doi.org/10.1007/s40831-021-00394-8, 2021.
- Yuan, W., Wang, X., Lin, C. J., Wu, F., Luo, K., Zhang, H., Lu, Z., and Feng, X.: Mercury uptake, accumulation, and translocation in roots of subtropical forest: implications of global mercury budget, Environ. Sci. Technol., 56, 14154–14165, https://doi.org/10.1021/acs.est.2c04217, 2022.
- Zhao, L., Anderson, C. W. N., Qiu, G., Meng, B., Wang, D., and Feng, X.: Mercury methylation in paddy soil: source and distribution of mercury species at a Hg mining area, Guizhou Province, China, Biogeosciences, 13, 2429–2440, https://doi.org/10.5194/bg-13-2429-2016, 2016.
- Zhao, H., Yan, H., Zhang, L., Sun, G., Li, P., and Feng, X.: Mercury contents in rice and potential health risks across China, Environ. Int., 126, 406–412, https://doi.org/10.1016/j.envint.2019.02.055, 2019.
- Zhao, L., Meng, B., and Feng, X.: Mercury methylation in rice paddy and accumulation in rice plant: a review, Ecotox. Environ. Safe., 195, 110462, https://doi.org/10.5194/bg-13-2429-2016, 2020.
- Zhou, J. and Obrist, D.: Global mercury assimilation by vegetation, Environ. Sci. Technol., 55, 14245–14257, https://doi.org/10.1021/acs.est.1c03530, 2021.
- Zhou, J., Obrist, D., Dastoor, A., Jiskra, M., and Ryjkov, A.: Vegetation uptake of mercury and impacts on global cycling, Nat. Rev. Earth Environ., 2, 269–284, https://doi.org/10.1038/s43017-021-00146-y, 2021.